Invited Paper

Fluorescence Lifetime Microscopy: A Stimulated-Emission Approach

Enrico Gratton, Chen Y. Dong and Peter T. C. So

Laboratory for Fluorescence Dynamics, Department of Physics,
University of Illiniois at Urbana-Champaign, IL 61801

Abstract

The stimulated emission process has been rarely exploited in spectroscopy and microscopy. Instead, a spectroscopy method based on the pump-probe principle has been frequently used to observe picosecond and femtosecond processes. This common approach has not been applied to microscopy due to the relatively slow acquisition time and the lack of three-dimensional information. We have exploited an idea originally proposed by F. Lytle group[28] in which two pulsed lasers are simultaneously focused on the sample. One laser is used to excite a population of molecules and the second laser to induce stimulated emission. The stimulated radiation is carried away in the same direction of the stimulating laser beam. By collecting the fluorescence emission in other directions, we observe a modulation of the fluorescence signal as a funtion of the delay between the two laser pulses. The repetition rate of the two lasers is slightly different producing a frequency beating at the laser overlapping volume. We have extended this method to achieve very high spatial and temporal resolution in the microscope environment. By recording only the beating frequency, we obtain a 3-D sectional effect similar to two-photon excitation. The harmonic content of the beating signal is limited by the laser pulse width and by the sample frequency response. Information of picosecond processes are extracted by standard frequency-domain methods. Using this principle, we built a stimulated emission microscope that has 3-D and fluorescence lifetime capabilities.

KEYWORDS: microscopy, stimulated-emission, spatial resolution, time-resolved imaging, pump-probe, frequency domain

2. Introduction

Time-resolved pump-probe spectroscopy is routinely used to study ultra-fast phenomena in biological systems. Important systems such as photosynthetic reaction centers, the visual protein rhodopsin, and heme proteins exhibit functionally important processes on femtosecond and picosecond time scales[1-3]. This paper introduces the application of pump-probe spectroscopy techniques to time-resolved microscopy. In addition to the well known advantages associated with traditional time-resolved microscopy[4-6], pump-probe microscopy can facilitate functional studies of ultra-fast protein reactions and motions in native environments, i.e. cells and tissues.

Pump-probe spectroscopy uses a pump pulse to promote the sample to an excited state, and then monitors the relaxation back to the ground state with a probe pulse. In the stimulated-emission approach, after a sample is excited (pumped), a probe beam is applied to cause stimulated emission. As the excited molecules relax, the probability for stimulated emission decreases until the excited state population is completely depleted. Measurements using stimulated emission can either directly observe the stimulated emission, or the resulting change in fluorescence intensity. In the work presented here, the fluorescence intensity is the experimentally observed quantity. To monitor the time course of molecular relaxation, the time between pump and probe pulses reaching the sample is varied, typically using a variable delay line in the time domain. The main purpose of pump-probe experiments is to measure ultra-fast relaxation by exploiting the inherent time resolution of ultrashort laser pulses without the need of ultra-fast optical detectors. Microchannel plates with about 20 GHz bandwidth are the fastest available detectors but they are inherently limited by the speed of electronic responses. For pump-probe experiments, the time resolution is essentially given by the pulse width of the laser, which has bandwidth on the order of hundreds of GHz to THz. At present, the shortest pulse width achieved is less than 10 fs[7]. For the probe beam to monitor the sample populations excited by the pump beam, it is necessary that the two beams overlap at the sample. A pump-probe signal is generated only from the part of the sample where the two beams coincide spatially and provides 3-D resolution.

Different approaches of time-resolved fluorescence microscopy have been devised for over two decades; all of these techniques relied on gated fast detectors. The development of time-resolved microscopy started with single point measurements using time-domain single photon counting[8,9]. Methods have since been developed, two of which are mentioned here, to image entire cells. The first method uses charge coupled device (CCD) cameras equipped with gain

0-8194-2052-2/96/$6.00

modulated image intensifiers to collect data simultaneously over the whole image. Both frequency-domain[4,6,10-15] and time-domain[16] versions have been constructed. The other approach modifies traditional confocal scanning microscopes and obtains time-resolved information on a point-by-point basis[5,17] with fast photomultipliers or microchannel plates. These conventional time-resolved microscopes are limited to the nanosecond regime because of slow detector responses.

The development of a pump-probe fluorescence microscopy can potentially increase the time-resolution of lifetime microscopy into the range of picoseconds and femtoseconds[18,19]. Today the ultrafast dynamics of photosystems or heme groups are investigated at the molecular level in solution[20-23]. A few pioneering time-resolved studies of these fast systems in whole cells are the exceptions[24]. Using pump-probe microscopy, ultra-fast spectroscopy of biological molecules can be performed in their native surroundings. Moreover, many interesting cellular systems with dynamics in the low nanosecond time range were studied at the limit of conventional time-resolved microscope technology. These slower studies should benefit from over two orders of magnitude time resolution improvement using the pump-probe approach. The monitoring of rotational diffusion in cytoplasm and membranes is an important example[25]. An improvement in time-resolution would allow picosecond rotational components to be resolved providing accurate micro-viscosity information in cellular organelles. Another application is the use of time-resolved resonance energy transfer to monitor protein aggregation in cell membrane or organelles[26,27]. Faster instruments can be used to study energy transfer over smaller distances and better characterize distance distribution between energy transfer pairs.
In this paper, we will start with a review of the theory of fluorescence pump-probe spectroscopy in the frequency domain. In particular, a heterodyning method using two asychronous laser sources will be presented. A major benefit of applying pump-probe fluorescence techniques in microscopy is the improvement in the image spatial resolution. The theoretical analysis of the point spread function will be presented. The essential components of the experimental apparatus for pump-probe spectroscopy in the frequency domain will be presented. The additional optics and electronics required to adopt pump-probe spectroscopy to the fluorescence microscope will also be described. Finally, the spatial and temporal resolution of the frequency domain pump probe technique will be evaluated. The power of this new instrument will be illustrated in examples of cellular lifetime resolved images using pump-probe methods.

3. Theoretical Basis

Pump-probe techniques are well established in the time-domain. In the frequency domain, the same concept can be applied to better utilize the harmonic content of pulsed lasers. This method was first demonstrated by F. Lytle[28,29]. One of the important advantages of implementing pump-probe method in the frequency-domain is the elimination of slow moving mechanical delay lines and the automation of the data acquisition processes. This important simplification permits easy integration of the pump-probe technique for use in microscopy. Pump-probe spectroscopy in the frequency-domain requires the use of intensity modulated light sources. In the simplest case, the light source is sinusoidally modulated. Pulsed excitation is composed of multiple sinusoidal Fourier components and will be discussed later. For chromophores with a single exponential lifetime τ, concentration c, quantum efficiency q, and cross section σ, $F(\vec{r},t)$, the density of fluorescence photons at position, $\vec{r}$, and time, t, obeys the differential equation:

$$\frac{dF(\vec{r},t)}{dt} = -\frac{1}{\tau}F(\vec{r},t) + cq\sigma I(\vec{r},t) \qquad (1)$$

$I(r,t)$ is the excitation photon flux which is sinusoidal with modulation frequency ω, modulation depth m_e. Separating spatial and temperal parts, $I(r,t) = [1 + m_e \sin(\omega t + \phi)I(r)$. The fluorescence signal F($\vec{r}$,t) is proportional to the excited state population, E($\vec{r}$,t).

The integrated fluorescence signal responds at the same angular frequency as the excitation, but with a phase delay, ϕ, and decreased modulation, m_f, due to the lifetime of the fluorescent sample:

$$F(t) \propto cq\sigma(1 + m_f \sin(\omega t + \phi)\int I(r)d^3r \qquad (2)$$

where c is chromophore concentration (assumed constant for simplicity), and σ is the absorption cross-section.

In solving Eqns. (1) and (2) and in the absence of saturation, the lifetime from the phase delay, ϕ, and modulation, m_f, can be determined:[30]

$$\tan(\phi) = \omega\tau \tag{3}$$

$$M = \frac{1}{\sqrt{1+\omega^2\tau^2}} \tag{4}$$

To generate stimulated emission, a sinusoidally modulated probe beam of intensity: $I'(\vec{r},t) = I(\vec{r})I(t) = I(\vec{r})[1+m_e' \sin(\omega' t+\phi')]$, is introduced. The repetition rates of the two lasers are slightly offset from each other, causing a variable delay between the pump and probe pulses. The effect of this delay is to repeatedly sample (probe) the population of the molecular ground state (excited state) at multiple times after the pump beam excitation.

We will make two assumptions at this point. First, the attenuation of both the pump and probe beam by the sample is negligible. This may not be true for conventional pump-probe spectroscopy but is certainly valid for a micron thick sample. Second, the dynamics of either the ground or excited state populations are slow compared to the transit time of light through the sample. For a sample with a thickness on the order of microns, the transit time is on the order of 1-10 fs.

In stimulated emission measurements, the amount of stimulated emission is dependent upon the transient excited state population E($\vec{r}$,t). The detected signals can be expressed as:

$$\Delta F(t) \propto \int \sigma' I'(\vec{r},t) E(\vec{r},t) d^3r \tag{5}$$

where σ' is the stimulated emission cross section. The time dependent ground and excited state populations can be deduced from equation (1) to (4). Neglecting constant terms, the previous equation can simplified and all time dependent terms isolated:

$$\Delta F(t) \propto cq\sigma\sigma'[1+m_e'\sin(\omega' t+\phi')][1+m_e \frac{1}{\sqrt{1+\omega^2\tau_m^2}} \sin(\omega t+\phi)] \int I(\vec{r}) I'(\vec{r}) d^3r \tag{6}$$

The temporal product term in Eqn. (6) may be rewritten as two terms containing the sum and difference of frequencies, respectively. If the frequencies of the pump and probe beams are $\Delta\omega = |\omega'-\omega|$ apart, then Eqn. (6), and therefore the detected fluorescence, contains a low-frequency, cross-correlation term which contains equivalent temperal information as the original signal:

$$\Delta F(t) \propto cq\sigma\sigma' m_e m_e' \frac{1}{\sqrt{1+\omega^2\tau_m^2}} \cos[|\omega'-\omega| t + (\phi'-\phi)] \int I(\vec{r}) I'(\vec{r}) d^3r \tag{7}$$

With electronic filtering, the cross-correlation signal can be isolated, and lifetime of the sample at the excitation volume can be accurately measured from the amplitude and phase of the signal.

Superior time-resolution is not the only distinctive advantage of pump-probe microscopy. Pump-probe microscopy also has an inherent 3-D sectioning capability and a spatial resolution comparable to the confocal method.

The effective spatial resolution in a microscopic fluorescence imaging system depends on the focusing of the excitation source and collection of the fluorescence signal. For an incoherent fluorescence imaging system using a large detector, the image at the object space F is given by

$$F = |h|^2 \otimes f \tag{8}$$

where h is the amplitude point spread function of the focusing lens, f is the spatial distribution of the fluorescence sample, and $\otimes$ represents the three dimensional convolution operation[31,32].

In the pump-probe system described by Eqns. (7), the spatial dependence of the cross-correlation signal depends on the overlap integral of the pump and probe intensity involved in the transition

$$\int I(\bar{r})I'(\bar{r})d^3r \tag{9}$$

The point spread function (PSF) is the integrand of Eqn. (9). Different pump and probe mechanisms can result in different intensity profiles near the focal point. For example, in a one-photon pump (1 pu) and one-photon probe (1 pr) system using the same wavelength, the PSF is

$$I_{1pu,1pr}(u,v) = I(u,v)I'(u,v) \tag{10}$$

where $I(u,v) = \left|2\int J_0(v\rho)e^{-\frac{1}{2}iu\rho^2}\rho d\rho\right|^2$ is the intensity distribution of light with wavelength λ near the focal point of a circular objective with numerical aperture sin(α). $u = 4k\sin(\frac{\alpha}{2})^2 z$ and $v = k\sin(\alpha)r$ are the dimensionless radial and axial coordinates respectively and, $k = \frac{2\pi}{\lambda}$ is the magnitude of the wave vector[33]. In our analysis, we have assumed for simplicity that the pump laser, probe laser, and signal detection are at the same wavelength. This assumption is reasonable since for a typical chromophore, a spectral band width of 100 nm is sufficient to include the wavelengths used in pump-probe microscopy. Further improvements in pump-probe fluorescence microscopy can be achieved if confocal detection is used. The point spread functions for the various pump-probe microscopy cases then become

$$I_{c,1pu,1pr}(u,v) = I(u,v)I'(u,v)I(u,v) \tag{11}$$

Pump-probe microscopy effectively rejects the background fluorescence contribution from off-focal axial planes. The question addressed is how much cross-correlation signal is detected from off-focal planes compared to conventional microscopy. To answer this question, we need to integrate Eqns. (10) over the radial coordinate and then compare the signal at each axial position. For conventional microscopy, the normalized fluorescence from each axial plane of interest is[31]

$$F_{axial}(u) = \frac{\int_0^\infty I(u,v)vdv}{\int_0^\infty I(0,v)vdv} \tag{12}$$

	Radial FWHM at u=0 (v)	Axial FWHM at v=0 (u)	Axial Depth Discrimination (FWHM, u)
1-photon	1.617	11.140	None
1-photon, confocal	1.160	8.020	8.510
1 -photon, pump/probe	1.160	8.020	8.510
1-photon, confocal, pump/probe	0.952	6.580	6.660

Table 1 Comparison of spatial resolution between conventional and pump-probe microscopy with non-confocal and confocal detection geometry.

Eqn. (12) may be applied to intensity profiles for pump and probe beams and the result, compared to the conventional microscopy. One sees that all versions of pump-probe microscopy offer better depth discrimination than conventional one-photon microscopy, which provides no depth discrimination due to the conservation of energy at different axial planes. By combining pump-probe techniques and confocal microscopy, greater background fluorescence rejection can be achieved.

The narrowest width is with the confocal one-photon pump-probe case; the FWHM is 6.66 u which is 0.783 of the width (8.51 u) in one-photon pump-probe and one-photon confocal. A spatial characteristics of pump-probe microscopy as compared with other methods is presented in Table 1.

4. Instrumentation and methods

In our implementation of pump-probe stimulated emission microscopy, we have designed our instrument around a high performance research microscope which features high excitation throughput and high collection efficiency (Fig. 1).

The most important components in any ultra-fast pump-probe experiment are the excitation light sources. In a frequency domain pump-probe experiment, two high repetition synchronous lasers with adjustable repetition rates are used. These lasers should have short pulse width, high peak power and low phase jitter. Two mode-locked neodymium-YAG (Nd-YAG, Antares, Coherent Inc., Santa Clara, CA) lasers are used. The Nd-YAG laser is either applied to the sample directly at 532 nm or synchronously pumps a DCM dye laser (Model 700, Coherent Inc., Santa Clara, CA) to obtain wavelengths from 580-680 nm. The typical repetition rate of the YAG lasers are 76.2 MHz but can be easily adjusted within a range of 5 KHz. A master synthesizer which generates a 10 MHz reference signal actively synchronizes the YAG lasers.

Glan Thomson polarizers are again used to control the laser power reaching the sample. The pump and probe laser beams are combined at a dichroic mirror (Chroma Technology Inc., Brattleboro, VT). The combined collinear laser beams enter the microscope system (Zeiss Axiovert 35, Thornwood, NY) deflected by a x-y scanner (Cambridge Technology, Watertown, MA). The scanning mirrors can be driven digitally. Each angular position is specified by a 8-bit binary number and results in images composed of 256x256 pixels. The epi-illuminated light path of the microscope has been modified to include a 10x eyepiece as the scan lens. It is positioned such that the x-y scanner is at its eye-point while the field aperture plane is at its focal point. The eyepiece has the proper optical property to linearly transform the angular deviation of the input laser beam controlled by the x-y scanner to a lateral translation of the focal point position at the field aperture plane. Since the field aperture plane is telecentric to the object plane of the microscope objective, the movement of the focal point on the object plane is proportional to the angular deviation of the scanned beam[34].

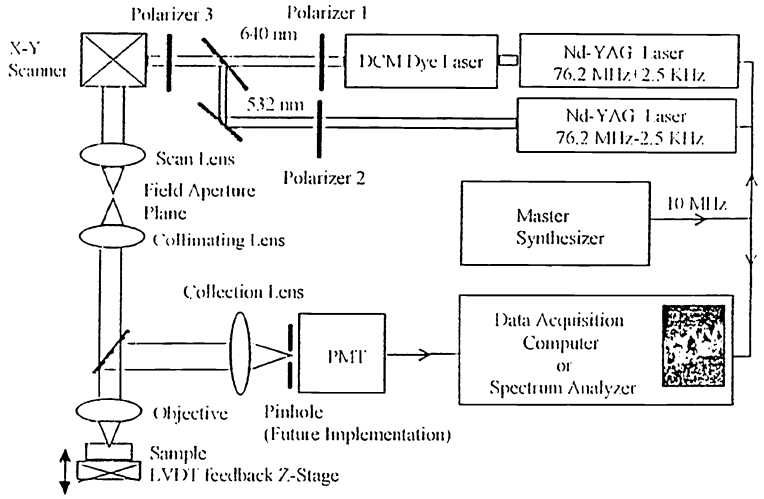

Fig. 1 Schematics of pump-probe stimulated emission microscope.

The combined beams are focused at the field aperture plane of the objective by the scan lens which ensures diffraction limited focused focusing at the object plane. After recollimination by the tube lens and deflected by a second dichroic mirror, both beams are directed to the objective. The objective used in these studies is a well-corrected, Zeiss 63x Plan-Neofluar with numerical aperture (NA) of 1.25. The pump and probe beams are focused onto a fluorescent sample and a modulated stimulated emission signal is generated. Quantum mechanics dictates that the stimulated emission photons propagate in the same direction as the probe beam photons, collinear with the pump beam photons. The remaining excited

state molecules emits fluorescent photons isotropically. Since the sum of photons emitted in stimulated emission mode and fluorescence mode is constant, equivalent information can be obtained by monitor either the fluorescence photons or the stimulated emission photons. We choose to detect the fluorescence photons as collected by the same objective in epi-illumination geometry. Since these fluorescence photons travel in the opposite direct of either the pump or probe beams which is largely free from the interference of the much stronger signals. Signal to noise ratio is significantly enhanced with this detection method. The fluorescence signal transmitted through the objective, the second dichroic mirror and two 640 nm bandpass filters is re-focused onto the detector (R928 or R1104 photomultiplier tube, Hamamatsu, Bridgewater, NJ).

For z-sectioning studies, it was necessary to vary the relative distance between the objective and the sample. Axial displacement of the objective is controlled by a stepping motor coupled to the objective manual adjustment mechanism and monitored by a linear variable differential transformer (LVDT, Schaevitz Engineering, Camden, NJ). This control system is designed to have a position resolution of 0.2 μm over a total range of 200 μm.

Using pulsed lasers, the frequency domain heterodyning method samples the complete temporal dynamics simultaneously. The cross-correlation frequency can be chosen for convenience, or to avoid noisy spectral regions. For microscopy, 5 KHz is used to maintain a reasonable frame acquisition rate. The cross-correlation signal is sent to a computer for analysis. The analog PMT signal is electronically filtered by a pre-amplifier (Stanford Research, Sunnyvale, CA) to isolate the cross-correlation signal. The filtered signal is then digitized by a 100 KHz, 12-bit sampling digitizer (A2D-160, DRA Laboratories, Sterling, VA). The Shannon sampling theorem dictates that at least two points per waveform need to be acquired to determine a sinusoidal signal. The determination of the n^{th} harmonic requires getting at least 2n time points within each time period of the cross-correlation frequency. For this first generation pump-probe microscope, only the first harmonic signal was acquired. In this case, only two points at each cross-correlation period are needed but we typically digitize four points per waveform to reduce harmonic noise. With four waveforms integrated per pixel, a pixel dwell time of 800 μs and a corresponding frame acquisition time of 52 s results for 5 KHz cross-correlation. After digital processing, the amplitude and phase of the cross-correlation signal are then displayed and stored by the data acquisition computer.

5. Spectroscopy Performance of Stimulated-emission Pump-probe Microscopy

5.1 Time-resolution of stimulated-emission pump-probe spectroscopy

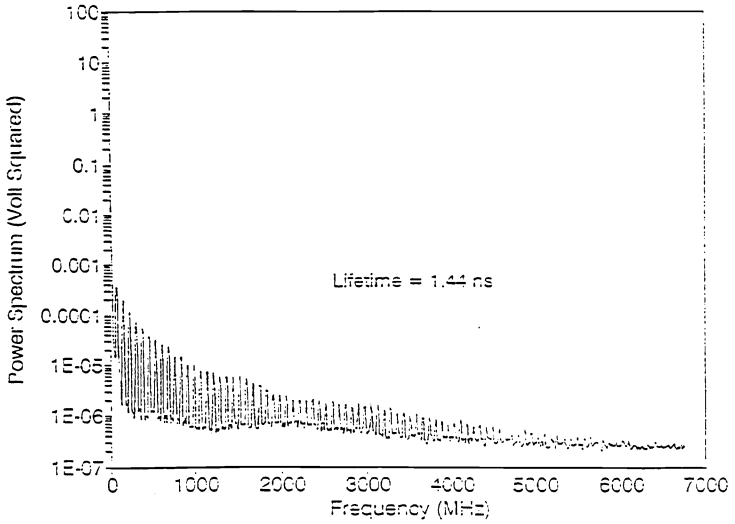

Fig. 2 Modulation versus excitation frequency for Rhodamine B in water as detected by frequency domain stimulated emission pump-probe technique

The dynamics of Rhodamine B in water was studied to characterize the time resolution of the microscope. In this case, the 532 nm YAG pump laser is operated at 76.2 MHz and the 610 nm DCM probe laser has repetition frequency of at 76.2 MHz + 210 Hz. Good signal to noise ratio at high cross-correlation harmonics of 8 GHz can be obtain with pump laser power of

35.6 μW and the probe laser power of 2.75 mW. The fluorescence signal was collected and optically filtered in the same manner as for imaging, and the photomultiplier signal is fed directly into a spectrum analyzer (HP 35655A, Hewlett Packet, Rolling Meadows, IL) where the harmonics are displayed and stored at a bandwidth of 16 Hz. The result of this measurement is presented in Fig. 2. A fluorescence lifetime of 1.4 ns was measured which is in agreement with the lifetime measured using a conventional fluorometer.

5.2 Lifetime measurement in the pump-probe microscopy

We obtained lifetime-resolved images of a mixture of 2.3 μm orange and 1.09 μm Nile-red (absorption maximum: 520 nm, emission maximum: 580 nm) fluorescent latex spheres (Molecular Probes, Eugene, OR). The two types of spheres were known to have different lifetimes. The measured lifetimes using standard frequency-domain phase fluorometry are 2.7 ns for 1.09 μm spheres and 4.3 ns for 2.3 μm spheres. In our images, the first harmonic amplitude and phase are measured (Fig. 3). The phase image was referenced to that of a 4.16 mM Rhodamine B slide for the purpose of lifetime calculations. From the histograms of lifetime values, the lifetimes of the spheres were determined to be 3.2 ± 1.0 ns (1.09 μm) and 4.2 ± 1.4 ns (2.3 μm). These values agree within error to the results from frequency-domain phase fluorometry.

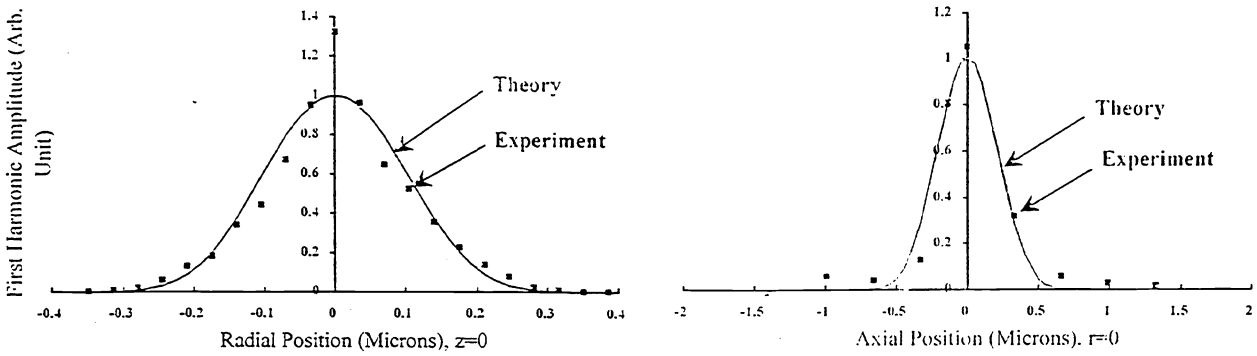

Fig. 3 A determination of pump-probe microscopy point spread function by imaging 0.28 μm orange fluorescent latex spheres:
(a) Radial intensity response. (b) Axial intensity response.

5.3 Experimental verification of pump-probe microscopy spatial resolution

To characterize the radial and axial spatial resolution of the system, orange fluorescent latex spheres of 0.28 μm in diameter (absorption maximum: 530 nm, emission maximum: 560 nm; Molecular Probes, Eugene, OR) were imaged. These spheres were immobilized between a cover slip and a flat microscope slide with Fluoromount G mounting medium (Southern Biotechnology, Birmingham, AL). The slide was left to dry at room temperature for one day before the spheres were imaged. The size of the spheres was uniform and calibrated by the manufacturer using electron microscopy. Since the dimension of the spheres are comparable to the FWHM of the theoretical pump-probe PSF at the wavelengths chosen, the fluorescence intensity measured is compared with the convolution of the theoretical PSF to the sphere size given by

$$I_{sphere}(z,r) = \frac{I(z,r)I'(z,r) \otimes S(z,r)}{I(0,0)I'(0,0) \otimes S(0,0)} \qquad (36)$$

where S(z,r) characterizes the physical dimension of the spheres in the axial (z) and radial (r) dimension; it has the value of 1 for $\sqrt{z^2 + r^2} \leq 0.14\mu m$, 0 otherwise. Data from 36 spheres were analyzed, and the experimental and theoretical intensity distributions are plotted in Fig. 4 While the axial data agree well with the Fraunhofer diffraction theory, there is

slight deviation of the radial data from the theoretical prediction. This deviation is probably due to slight misalignment of the pump and probe lasers. Other possible effects include chromatic aberrations and polarization effect of the focusing objective.

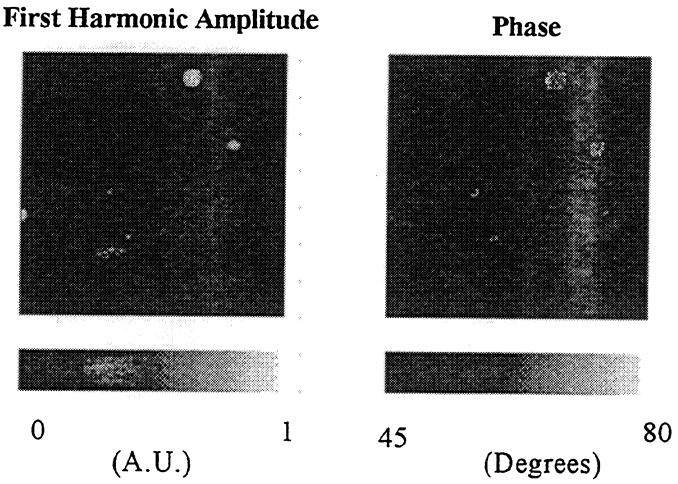

Fig. 4 Using pump-probe microscopy, time-resolved images of 1.09 μm Nile-red (τp= 3.2±1.0 ns) and 2.3 μm orange (τp= 4.2±1.4 ns) fluorescent latex spheres were obtained: (a) image of normalized first harmonic amplitude. (b) image of phase values in degrees.

5.4 Comparison Between Conventional Microscopy and Pump-Probe Fluorescence Microscopy in Human Erythrocytes and Mouse Fibroblasts.

To demonstrate the superior spatial resolution achieved by pump-probe fluorescence microscopy compared to conventional one-photon microscopy, we imaged two commonly used biological systems: human erythrocytes and mouse fibroblast cells.

The human erythrocytes were labeled with the membrane dye Rhodamine DHPE (Molecular Probes, Eugene, OR). A small amount of erythrocytes was mixed with Hanks Balanced Salt Buffer (HBSB with $NaHCO_3$) to make a 1 mL mixture. The solution was spun at 1000 rpm for 5 minutes before the top buffer was removed. The erythrocytes were then shaken and diluted to 1 mL with HBSB. 6 μL of Rhodamine DHPE (at 5 mg/mL DMSO) were injected into the solution containing the cells and allowed to incubate for 30 minutes. After incubation, the cells were again spun down and washed with HBSB two more times to remove residual dye before mounting onto a microscope slide. Nail polish was used to seal the coverslip.

The mouse fibroblast cells were grown on a coverslip. For fixation, they were placed in acetone for 5 minutes and allowed to air dry. Then, a few drops of a solution containing 10 μg/mL of Rhodamine DHPE (diluted in PBS, 0.1% Triton X-100) were placed onto the coverslip and incubated for 30 minutes. After incubation, the dye was removed by rinsing the coverslip in PBS buffer twice before mounting onto a flat microscope slide. For mounting, a drop of the mounting medium Prolong (Molecular Probes, Eugene, OR) was placed between the coverslip and a slide. In a few hours, the mounting medium dries and the slide was ready for viewing.

The images at the first harmonic of 5 KHz is presented in Fig.5 along with the corresponding one-photon images. The one-photon images were obtained by blocking the probe beam and recording only the fluorescence intensity due to the pump beam. In this manner, the cells were not moved relative to the microscope objective and a comparison between the two techniques can be made. From the image of the erythrocytes, it is apparent that the pump-probe images can better reject the fluorescence from off-focal planes. The one-photon images show much more background fluorescence from the central region of the erythrocytes than pump-probe microscopy. Similarly, the pump-probe image of the mouse fibroblast shows

superior spatial resolution compared to the corresponding one-photon image by revealing the finer details of the cell's structure.

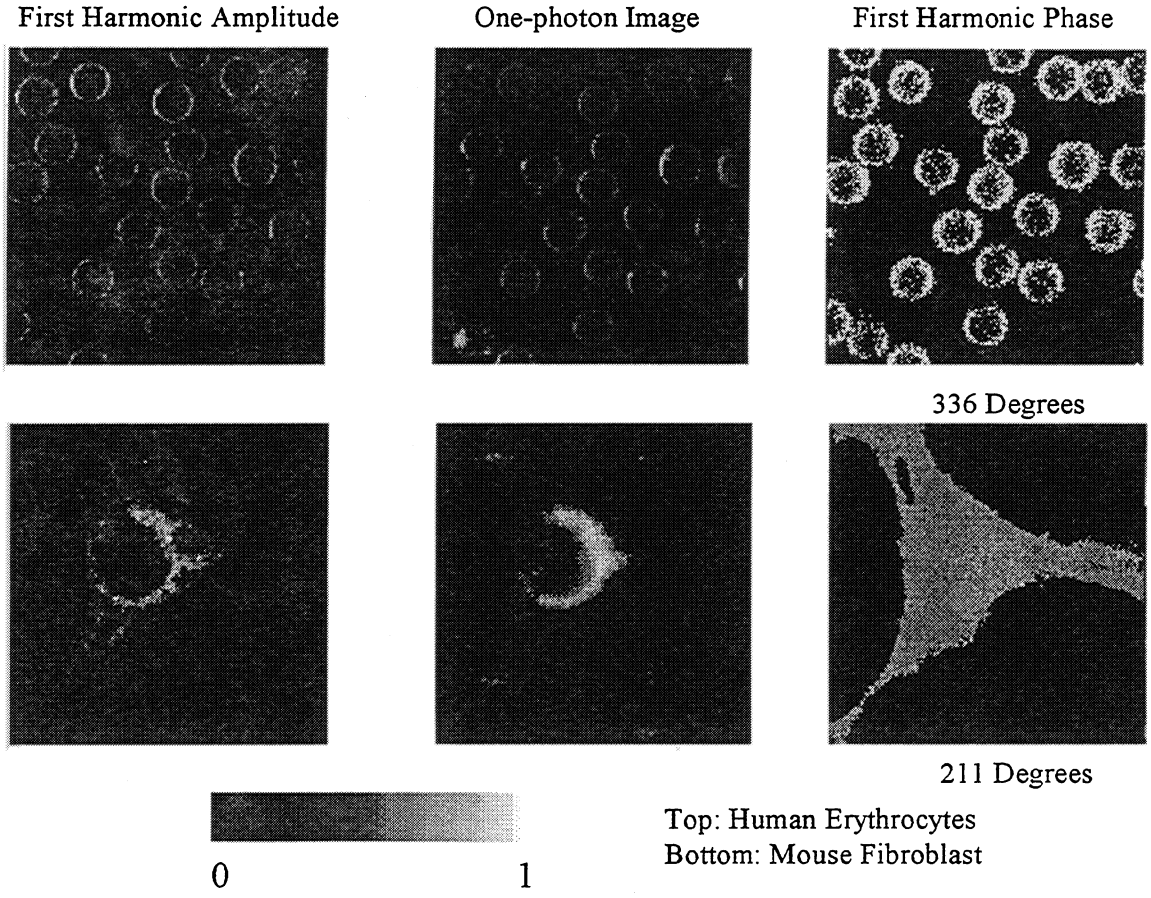

Fig. 5 Normalized first harmonic amplitude images using pump-probe microscopy is compared with intensity images using conventional laser scanning microscopy. (Top: Human Erythrocytes, Bottom: a Mouse Fibroblast Cell; Staining: Rhodamine DHPE)

6.5 Multiple dye labeling application

We examined mouse fibroblast cells doubly labeled with the nucleic acid stain ethidium bromide and the membrane stain Rhodamine DHPE (Molecular Probes, Eugene, OR). The pump-probe image is shown in Fig. 6. These cells (grown on a coverslip) are fixed and stained in the same manner as the mouse fibroblast cell discussed above. The only difference is that the coverslip was covered first with ethidium bromide (1 mM in PBS, 0.1% Triton X-100) for 30 minutes and then stained by Rhodamine DHPE (10 μg/mL in PBS, 0.1% Triton X-100) for another 30 minutes before it was rinsed twice in PBS and mounted for viewing. The lifetimes of the cytoplasmic and nuclear region were determined from the phase image. The reference phase was obtained from a slide of 4.16 mM Rhodamine B in water. It was found that the average and the full width at half maximum of lifetime histograms in the cytoplasm and nucleus are 2.0 ± 0.5 ns and 6.6 ± 4.8 ns, respectively. For comparison, the lifetime of Rhodamine B in water was determined from standard frequency-domain phase fluorometry to be 1.44 ns. Furthermore, the lifetimes of the unbound ethidium bromide and bound ethidium bromide to nucleic acid are 1.7 and 24 ns, respectively. Our measurements of lifetime in the cytoplasm show that there was significant staining of cytoplasmic structures by Rhodamine DHPE. The average lifetime in the nucleus is between that of bound and unbound ethidium bromide indicative of the fact that both populations of the chromophores exist in the nucleus. Nonetheless, the

lifetime contribution from bound ethidium bromide is sufficient to distinguish the different lifetimes in the nucleus and cytoplasm as demonstrated by the phase image. This example demonstrates one advantage of lifetime-resolved imaging. From intensity imaging, it is difficult to distinguish the cytoplasmic and nuclear regions since these chromophores have similar emission spectra. With lifetime imaging, sharp contrast between the two species of chromophores can be generated.

7. Conclusion

We have demonstrated the first application of the stimulated emission technique to fluorescence microscopy. By measuring the fluorescence signal at the cross-correlation frequency, pump-probe fluorescence microscopy can provide superior spatial resolution and effective off-focal background rejection compared to conventional one-photon microscopy. Due to the wavelengths used in the one-photon pumping and probing processes, this technique has better spatial resolution than two-photon excitation microscopy, and comparable spatial resolution to confocal microscopy. Furthermore, imaging at low-frequency harmonics eliminates the need of using a fast optical detector in time-resolved imaging of biological systems. The technical development of pump-probe microscopy is still in its early stages. Substantial future improvements are expected. The implementation of transient absorption mode in pump-probe microscopy will allow ground state kinetics to be directly monitored. The addition of two-photon excitation would improve the microscope spatial resolution as well as making wavelength dependent spectroscopy possible. The implementation of the pump-probe technique in the time-domain would make the microscopy alignment and automation more difficult but may take time-resolved microscopy solidly into the femtosecond time scale. The pump-probe microscopy technique has the potential to radically transform the field of time-resolved microscopy.

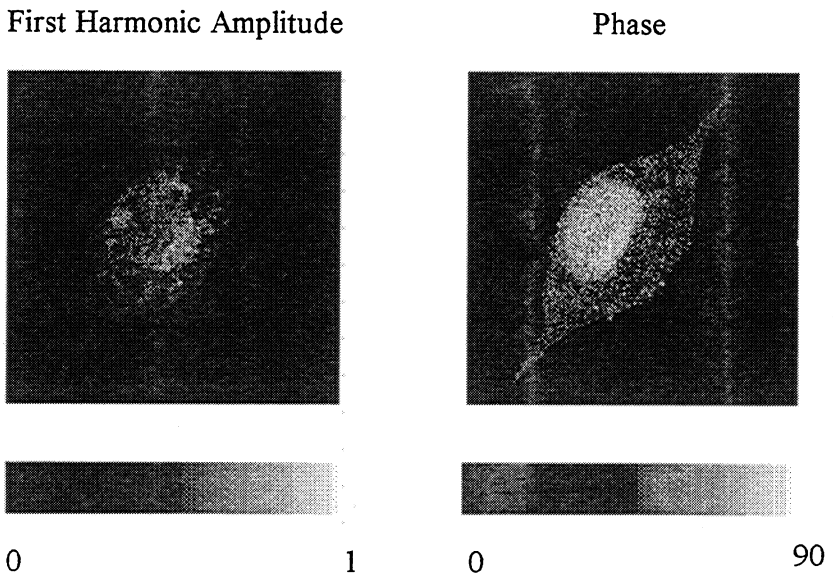

Fig. 6 Time-resolved Images of a mouse fibroblast cell labeled with Rhodamine DHPE and Ethidium Bromide (Membrane and cytoplasm: τp= 2.0±0.5 ns, Nucleus: τp= 6.6±4.8 ns). Images of normalized first harmonic amplitude and phase in degree were shown.

8. Acknowledgment

We would like to thank Dr. Matt Wheeler, Dr. Laurie Rund, Ms. Linda Grum, and Ms. Melissa Izard for providing us with mouse fibroblast cells. This work was supported by the National Institute of Health (RR03155).

9. References

1. M. A.El-Sayed, I. Tanaka, and Y. Molin, ed., *Ultrafast Process in Chemistry and Photobiology*, Blackwell Scinece, Oxford England (1995)
2. W. Kaiser, ed., *Ultra-short Laser Pulses: Generation and Applications,* Springer-Verlag, New York (1993)
3. R. M. Hochstrasser, and C. K. Johnson, Biological Processes Studied by Ultrafast Laser Techniques, 357-417 in *Ultrashort Laser Pulses.* (W. Kaiser, ed.) Springer-Verlag, New York (1988).
4. G. Marriott, R. M. Clegg, D. J. Arndt-Jovin, T. M. Jovin, *Time resolved imaging microscopy* Biophys J 60 1347-1387 (1991).
5. E. P. Buurman, R. Sanders, A. Draaijer, H. C. Gerritsen, J. J. F. Van Veen, P. M. Houpt and Y. K. Levine, *Fluorescence Lifetime Imaging Using a Confocal Laser Scanning Microscope,* Scanning 14, 155-159 (1992).
6. J. R. Lakowicz, H. Szmacinski, K. Nowaczyk and M. L. Johnson, *Fluorescence lifetime imaging of calcium using Quin-2,* Cell Calcium 13, pp 131-147 (1992).
7. J. Zhou, G. Taft, C. P. Huang, I. P. Christov, H. C. Kapteyn, and M. M. Murnane, *Sub-10 fs Pulse Generation in Ti:Sapphire: Capabilities and Ultimate Limits.* 39-40 in *Ultrafast Phenomena IX.* (P. F. Barbara, W. H. Knox, G. A. Mourou, and A. H. Zewail ed.) Springer-Verlag, Berlin (1994)
8. J. A. Dix, and A. S. Verkman, *Pyrene Excimer Mapping in Cultured Fibroblasts by Ratio Imaging and Time-Resolved Microscopy*, Biochem. 29, 1949-1953 (1992).
9. S. M. Keating, and T. G. Wensel, *Nanosecond Fluorescence Microscopy: Emission Kinetics of Fura-2 in Single Cells*, Biophys. J. 59, 186-202 (1990).
10. J. R. Lakowicz, H. Szmacinski, K. Nowaczyk, K. W. Berndt and M. L. Johnson M L, Fluorescence lifetime imaging, Anal Biochem 202 316-330 (1992).
11. M. vandeVen M and E. Gratton in *Optical Microscopy: Emerging Methods and Applications* New York: Academic Press 373-402 (1993.
12. W. W. Mantulin, T. French and E. Gratton E *Optical imaging in the frequency domain* 158-166 in *Proc.* SPIE, *Medical Lasers and Systems II* 1892 (D. M. Harris ed.) (1993).
13. P. T. C. So, T. French and E. Gratton *A frequency domain time-resolved microscope using a fast-scan CCD camera* 83-92 in *Proc.* SPIE, *Time-Resolved Laser Spectroscopy IV* 2137 (J R Lakowicz ed.) (1994).
14. J. R. Lakowicz, H. Szmacinski and M. L. Johnson, *Calcium imaging using fluorescence lifetimes and long-wavelength probes,* Journal of Fluorescence 2, 47-62 (1992).
15. D. W. Piston, D. R. Sandison and W. W. Webb, *Time-Resolved Fluorescence Imaging and Background Rejection by Two-Photon Excitation in Laser Scanning Microscopy* 379-389 in *Proc* SPIE 1640 (1992).
16. T. Oida, Y. Sako and A. Kusumi, *Fluorescence lifetime imaging microscopy (filmscopy),* Biophys J 64, 676-685 (1993)
17. C. G. Morgan, A. C. Mitchell and J. G. Murray, *Prospects for confocal imaging based on nanosecond fluorescence decay time,* J of Microscopy 165, 49-60 (1991).
18. C. Y. Dong, P. T. C. So, T. French and E. Gratton, *Fluorescence Lifetime Imaging by Asynchronous Pump-Probe Microscopy*, Biophy. J. In press
19. C. Y. Dong, P. T. C. So and E. Gratton, *Spatial Resolution in Scanning Pump-Probe Fluorescence Microscopy* , Applied Optics, Submitted.
20. Y. W. Jia, D. M. Jonas, T. H. Joo, Y. Nagasawa, M. J. Lang and G. R. Fleming, *Observation of Ultrafast energy transfer from the accessory bacteriochlorophylls to the special pair in photosynthetic reaction centers,* J. Phys. Chem 99, 6263-6266 (1995)
21. M. Du, X. L. Xie, L. Mets, G. R. Fleming, *Direct Observation of Ultrafast Energy Transfer Process in Light Harvesting Complex,* J. Phys. Chem 98, 4736-4741 (1994).
22. S. Savikhin, P. I. Vannoort, Y. W. Zhu, S. Lin, R. E. Blankenship and W. S. Struve, *Ultrafast Energy Transfer in Light-Harvesting Cholorosomes from The Green Sulfur Bacterium Chlorobium Tepidum,* Chemical Physics 194, 245-258 (1995).
23 T. Q. Lian, B. Locke, Y. Kholodenko, and R. M. Hochstrasser, *Energy Flow from Solute to Solvent Probed by Femtosecond IR Spectroscopy - Malachite Green and Heme Protein Solutions,* J. Phys. Chem. 98, 11648-11656 (1994)

24 D. Foguel, R. M. Chaloub, J. L. Silva, A. R. Crofts, and G. Weber, *Pressure And Low Temperature Effects on the Fluorescence Emission Spectra and Lifetimes of the Photosynthetic Components of Cyanobacteria,* Biophys. J., 63, 1613-1622 (1992).

25 H. P. Kao, J. R. Abney, and A. S. Verkman, *Determinants of the Translational Mobility of a Small Solute in Cell Cytoplasm*, J. Cell Biol. 120 175-184 (1993).

26.T. W. J. Gadella and T. M. Jovin, *Oligomerization of Epidermal Growth Factor Receptors on A431 Cells Studied by Time-resolved Fluorescence Imaging Microscopy -- A Stereochemical Model for Tyrosine Kinase Receptor Activation,* J. Cell Biol. 129, 1543-1558 (1995).

27. X. F. Wang, A. Periasamy, G. W. Gordon, P. Wodnicki and B. Herman, *Fluorescence Lifetime Imaging Microscopy (FLIM) and its Applications,* 64-76 in *Time-Resolved Laser Spectroscopy in Biochemistry IV,* (J. R. Lakowicz, ed.), *Proc.* SPIE 2137, (1994).

28. P. A. Elzinga, R. J. Kneisler, F. E. Lytle, G. B. King, and N. M. Laurendeau, *Pump/Probe Method for Fast Analysis of Visible Spectral Signatures Utilizing Asynchronous Optical Sampling* ,Applied Optics 26, 4303-4309 (1987).

29. P. A. Elzinga, F. E. Lytle, Y. Jian, G. B. King, and N. M. Laurendeau, *Pump/Probe Spectroscopy by Asynchronous Optical Sampling*, Applied Spectroscopy 41, 2-4.(1987).

30. J. R. Lakowicz, P*rinciples of Fluorescence Spectroscopy,* New York, Plenum Press (1983).

31. T. Wilson and C. Sheppard, *Theory and Practice of Scanning Optical Microscopy,* London, Academic Press Inc. Ltd. (1984).

32. T. Wilson, ed., *Confocal Microscopy.* London: Academic Press Ltd. (1990).

33. M. Born and E. Wolf *Principles of Optics.* 5th ed. Oxford, Pergrmom Press, (1985).

34. E. H. K. Stelzer *The Intermediate Optical System of Laser-Scanning Confocal Microscopes* 139-153 in *The Handbook of Biological Confocal Microscopy.* (Pawley J. ed), New York, Plenum Press, (1995).